RSC Advances

ROYAL SOCIETY OF CHEMISTRY

www.rsc.org/advances

DNA/BSA binding, DNA cleavage and electrochemical properties of new multidentate copper(II) complexes

Elumalai Sundaravadivel[a], Sairaj Vedavalli[a], Muthusamy Kandaswamy[a]*, Babu Varghese[b], Perumal Madankumar[c]

E-mail: mkands@yahoo.com

*[a]*Department of Inorganic Chemistry, University of Madras, Guindy Campus, Chennai 600 025, India*

*[b]*Sophisticated Analytical Instruments Facility, Indian Institute of Technology, Chennai 600 036, India*

*[c]*Department of Biochemistry, University of Madras, Guindy Campus, Chennai 600 025, India*

*corresponding author
E-mail: mkands@yahoo.com
Tel: +91-44-22351269 Fax: +91-44-22300488

Abstract: New series of multidentate copper(II) complexes $[Cu(L^{1-5})](ClO_4)$(**1** - **5**) were synthesized [where L^{1-5} represent [N-(salicylaldimine)-N'-[(2-formyl-4-bromo-6-(4-methylpiperazine-1-yl)methyl)phenol] diamines; diamines *viz*., L^1-1,2-diamino ethane, L^2-1,3-diamino propane, L^3-1,2-diamino benzene, L^4-2-aminobenzylamine and L^5-1,8-diamino naphthalene] and characterized by elemental analysis and spectroscopic methods. The single crystal X-ray diffraction analysis shows that the multidentate copper(II) complex (**1)**, in which the copper atom exhibits a distorted square planar geometry, coordinates with two phenolic oxygen atoms and two ethylenediamine nitrogen atoms. The assembly of molecular constituents exhibits interesting supramolecular architecture through the C-H…O interactions forming a two dimensional supramolecular sheets, extending infinitely along the (1 0 0) plane. The channels thus farmed are large sufficient enough to hold the guest (solvent) molecules. Cyclic voltammogram of these copper(II) complexes exhibit one quasi reversible reduction wave in the cathodic region. The DNA/BSA binding, DNA cleavage, antimicrobial activity and MTT assay of these complexes were investigated. The binding propensities of the complexes toward calf thymus DNA(CT DNA) were also investigated by UV and Fluorescent spectroscopy, Viscosity measurements and Circular Dichoric spectral studies. The binding constant (K_b) values are in the range of 0.84 X 10^4 - 3.0 X 10^4 M^{-1} and apparent binding constants (K_{app}) in range from 1.9 X 10^6 M^{-1} to 4.2 X 10^6 M^{-1} as measured by UV and Fluorescent methods. The cleavage activities are in the following order (**5**) > (**4**) > (**3**) > (**1**). The mechanistic investigation suggests that singlet oxygen plays a vital role in the cleavage process. All the copper(II) complexes (**1-5**) exhibit significant interaction with Bovine Serum Albumin (BSA) and the results show that the binding mechanism is a static quenching process.

Keywords: Multidentate copper(II) complexes, DNA/BSA binding studies, DNA cleavage studies, MTT assay, antimicrobial activity.

1. Introduction

Interactions of small molecules with specific DNA sequences have been studied for several decades in the hope of learning design principles to control gene expression.[1] Over the past years, DNA has been used as a traditional target in chemotherapy for human cancer. Platinum(II) complexes are widely used as metal based drugs for cancer therapy. In this co-nnection, Cisplatin (*cis*-diamminedichloroplatinum(II)) is one popular drug, which inhibits the proliferation of cancer cells through binding with DNA. However, most of the platinum(II) complexes possess inherent limitations such as side effects and acquired resistance phenomena.[2] The high therapeutic efficiency of anticancer drugs has inspired the development of next generation agents that are effective against cancer cells with fewer side effects. Several studies show that the transition metal ions, especially the copper ions have strong interactions with DNA which result in conformational changes of the DNA structure.[3] Some results found that the copper is a competitive inhibitor of cisplatin uptake[4] and also it has been recognized as an essential trace element for living organisms. The interaction studies of schiff's base metal complexes with DNA and BSA are well known. It's much less common for the interaction of piperazine attached copper(II) complexes, owing to the piperazine molecule shows numerous physiological effect and screened its effects in antianginals, anti-cancer, antidepressant, anti-tuberculosis, antpsychotic, antidiabetic, hypolipidemic agent, flavouring agent and antihistamines.[5] Only few reports are available in the field of DNA/BSA binding and cleavage studies so for, using acyclic copper(II) complexes. Recently, our group reported that new methyl substituted acyclic copper(II) complexes have good activity for DNA binding and cleavage.[6]

Serum albumins are the major soluble proteins, which have many physiological functions such as the maintaining pH of blood, the osmotic pressure and acting as transporters for a variety of organic and inorganic compounds including metal ions.[7] BSA has been one of the most extensively studied, because of its structural homology with human serum albumin (HAS).[8] Significant interaction of any drug with a protein may result in the formation of a stable protein-drug complex, which has dominant role in storage and drug disposition.[9] Therefore studies on drug interaction with BSA are important to understand the storage, disposition, mechanism, pharmacokinetics and toxicity of the drug.

In this paper, we have described the synthesis and characterization of a series of bromo substituted acylic copper(II) complexes (Scheme 1). The mode of binding and binding affinity of copper(II) complexes to calf thymus (CT-DNA) was monitored using spectroscopic titration and viscosity measurements. *In vitro* MTT assay, antimicrobial activities and the reactivity towards BSA of the acylic copper(II) complexes are discussed. Nuclease activities of copper(II) complexes and mechanism of cleavage are also reported.

Scheme 1. Synthesis of new copper(II) complexes (1-5)

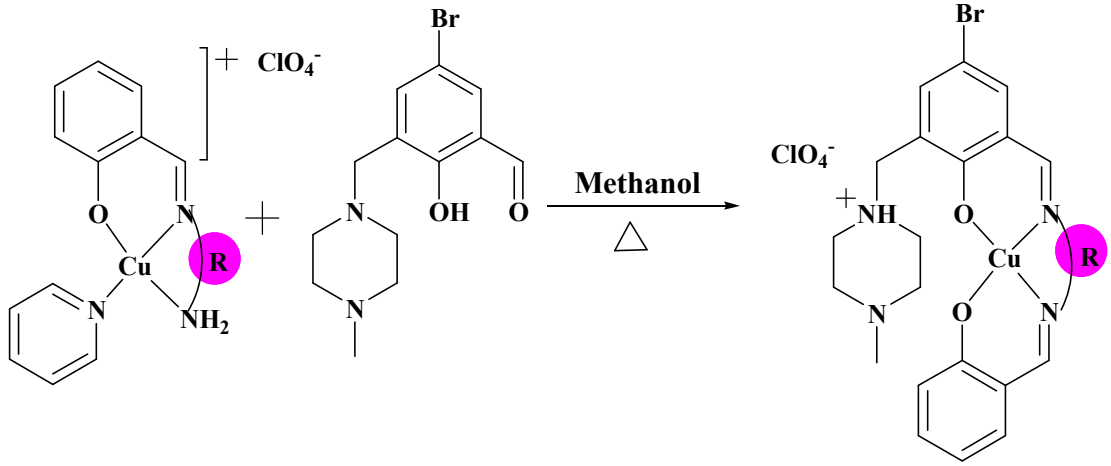

Complex	1	2	3	4	5
R	-(CH2)2-	-(CH2)3-			

2. Experiment

2.1 Materials and Methods

Precursor ligand 2-hydroxy-5-bromo-3-[(4-methylpiperazine-1-yl)methyl]benzaldehyde, precursor complexes (PC) [Cu(sal-diamines)(py)](ClO_4), (diamine- 1,2-diamino ethane(PC-I), 1,3-diaminopropane(PC-II), 1,2-diamino benzene(PC-III), 2-aminobenzylamine(PC-IV), 1,8-diamino naphthalene(PC-V)) were prepared based on the earlier reported methods.[6,10] Tetra(n-butyl)ammoniumperchlorate (TBAP) purchased from Fluka and recrystallized from hot methanol was used as the supporting electrolyte in electrochemical measurement, (Caution! TBAP is potentially explosive and hence, care should be taken in handling the compound). All other chemicals and solvents were purified by reported procedures.[11] CT DNA and pBR322 DNA and

Ethidium bromide (EtBr) were purchased from Bangalore Genie (India). Tris(hydroxymethyl)aminomethane-HCl (Tris-HCl) buffer was prepared using deionized water. 3-(4, 5-dimethylthiazol- 2-yl)-2, 5-diphenyl-2H-tetrazolium bromide (MTT) was purchased from Sigma chemical Co., (St. Louis, MO, USA). Dulbecco's Modified Eagle Medium (DMEM), fetal bovine serum (FBS), dimethyl sulfoxide (DMSO), phosphate buffered saline (PBS) and trypsin were purchased from Himedia laboratories (Mumbai, India).

Elemental analysis was carried out in Carlo Erba model 1106 elemental analyzer. FT-IR spectra were recorded in (4000 – 400 cm^{-1}) Perkin Elmer FTIR spectrometer with samples prepared as KBr pellets. UV–visible spectra were recorded using a Perkin Elmer Lambda 35 spectrophotometer operating in the range of 200–900 nm. Emission intensity measurements were carried out using Perkin Elmer LS-45 fluorescence spectrometer. Electrochemical measurements were performed using Electrochemical analyzer CHI 1008 using a three-electrode cell. glassy carbon electrode as the working electrode, saturated Ag/AgCl electrode as the reference electrode and platinum wire as auxiliary electrode. The concentrations of all the complexes were kept at 10^{-3} M. TBAP (10^{-1} M) was used as the supporting electrolyte to all electrochemical experiments. Electron spray ionization mass spectral (ESI-MS) measurements were performed by Thermo Finnegan LCQ-6000 Advantage Max-ESI mass spectrometer and acetonitrile as a solvent. Circular dichroism (CD) spectra were obtained on a JASCO J-715 spectropolarimeter.

X-ray diffraction intensity data for complex (**1**) was collected using a Bruker AXS Kappa APEX II single crystal CCD diffractometer equipped with graphite-monochromated Mo Kα radiation (λ = 0.71073 Å) at room temperature with crystal dimension of 0.25 X 0.2 X 0.15 mm^3. Accurate unit cell parameters were determined from the reflections of 36 frames measured in three different crystallographic zones by the method of difference vectors. The data collection,

data reduction and absorption correction were performed by APEX2, SAINT-plus and SADABS programs. The structure was solved by direct methods procedure using SHELXS-97 program and the non-hydrogen atoms were subjected to anisotropic refinement by full-matrix least squares on F^2 using SHELXL-97 program.[12] The bond distances of the disorder components were fixed using standard restraints. The atomic displacement parameters of the minor components were allowed to move equally with the major components using standard constraints. The positions of all the hydrogen atoms were identified from difference electron density map and were treated accordingly. The hydrogen atoms bound to the C atoms were allowed to ride on the parent atom with $U_{iso}(H) = 1.2U_{eq}(C)$ and $1.5U_{eq}(C)$.

2.2 Synthesis of copper(II) complexes

2.2.1 $[CuL^1](ClO_4)$ (1)

Copper(II) complex (**1**) was synthesized by adding the solid PC-I (0.405 g, 1 mmol) slowly to precursor ligand (2-formyl-4-bromo-6-[(4-methylpiperazine-1-yl)methyl] phenol) (0.312 g, 1 mmol) dissolved in 30 mL methanol and the mixture was refluxed for 3 h. The resulting solution was then filtered in hot condition and allowed to stand at room temperature. The dark blue color solid was obtained by evaporating the solution up to 10 mL at room temperature. For crystallization purpose the solid was dissolved in acetonitrile and on slowly evaporating the solution, the blue crystals obtained were collected and used for single crystal X-ray diffraction analysis. Yield: 0.46 g (74%); dark blue color solid; Anal.Cal for $C_{22}H_{26}BrClCuN_4O_6$: C, 42.52; H, 4.22; N, 9.02; Found: C, 42.43; H, 4.18; N, 8.93%; ESI-MS: displays a peak at m/z 520 (calculated m/z 520). Selected FT-IR (KBr, ν/cm^{-1}): 1635(s), 1094(s), 620(s). UV-visible in DMF [λ_{max}/nm (ε/M^{-1} cm^{-1})]: 578(110), 366 (128,000), 276(230,000).

2.2.2 $[CuL^2](ClO_4)$ (2)

Copper(II) complex (**2**) was prepared as a green solid by the method used for (**1**), where PC-II (0.419 g, 1 mmol) was used instead of PC-I. Yield: 0.45 g (71%); green solid; Anal.Cal for $C_{23}H_{28}BrClCuN_4O_6$: C, 43.48; H, 4.44; N, 8.82; Found: C, 43.41; H, 4.38; N, 8.78%; ESI-MS: displays a peak at m/z 534 (calculated m/z 534). Selected FT-IR (KBr, ν/cm^{-1}): 1619(s), 1088(s), 619(s). UV-visible in DMF [λ_{max}/nm (ε/M^{-1} cm^{-1})]: 586(312), 369(90,000), 278(166,000).

2.2.3 $[CuL^3](ClO_4)$ (3)

Brown colored complex (**3**) was prepared by the same procedure used for (**1**), where PC-III was used in place of PC-I, offered brown color solid. Yield: 0.42 g (63%); Brown solid; Anal.Cal for $C_{26}H_{26}BrClCuN_4O_6$: C, 46.65; H, 3.91; N, 8.37; Found: C, 46.58; H, 3.83; N, 8.31%; ESI-MS: displays at m/z 568 (calculated m/z 568). Selected FT-IR (KBr, ν/cm^{-1}): 1609(s), 1087(s), 621 (s). UV-visible in DMF [λ_{max}/nm (ε/M^{-1} cm^{-1})]: 608(500), 344(64,000), 248(110,000).

2.2.4 $[CuL^4](ClO_4)$ (4)

Copper(II) complex (**4**) was prepared by the method used for (**1**), where PC-IV was used in place of PC-I, offering green color solid. Yield: 0.5 g (73%); Green color solid; Anal.Cal for $C_{27}H_{28}BrClCuN_4O_6$: C, 47.45; H, 4.13; N, 8.20; Found: C, 47.41; H, 4.09; N, 8.13%; ESI-MS: displays at m/z 582 (calculated m/z 582).Selected FT-IR (KBr, ν/cm^{-1}): 1607(s), 1097(s), 620(s). UV-visible in DMF [λ_{max}/nm (ε/M^{-1} cm^{-1})]: 612(230), 374(51,200), 280(71,000).

2.2.5 $[CuL^5](ClO_4)$ (5)

Copper(II) complex (**5**) was prepared by the method used for (**1**), where PC-V was used in place of PC-I, offering brown color solid. Yield: 0.42 g (59%); Brown color solid; Anal.Cal for $C_{30}H_{28}BrClCuN_4O_6$: C, 50.08; H, 3.92; N, 7.79; Found: C, 50.01; H, 3.88; N, 7.74%; ESI-

MS: displays a peak at m/z 618 (calculated m/z 618). Selected FT-IR (KBr, ν/cm^{-1}): 1636(s), 1096(s), 619(s). UV-visible in DMF [λ_{max}/nm (ε/M^{-1} cm^{-1})]: 603(230), 420(34,000), 307(48,300).

2.3 DNA binding experiments

Electronic absorption spectra were carried out at 25 ºC by fixing the concentration of the complexes (2 X 10^{-5} M), for various DNA concentrations ranging from 0 to 25 X 10^{-5} M. The absorption spectra measurements were carried out in the range of 200 to 400 nm, using DNA in Tris-HCl buffer solution (50 mM Tris-HCl buffer, pH = 7.2) as reference. The binding constants (K_b) were determined from the spectroscopic titration data using the following equation(1):

$$[DNA]/\varepsilon_a-\varepsilon_f = [DNA]/\varepsilon_b-\varepsilon_f + 1/K_b\ (\varepsilon_b-\varepsilon_f) \quad (1)$$

The 'apparent' extinction coefficient (ε_a) was obtained by calculating A_{obs}/[Cu]. The terms ε_f and ε_b correspond to the extinction coefficients of free (unbound) and the fully bound complexes. The binding constant (K_b) was calculated using a plot of [DNA]/ ($\varepsilon_a - \varepsilon_f$) vs [DNA] from the ratio of slope to intercept.[13]

Fluorescence quenching experiments were carried out by addition of complexes to sample solution containing EtBr-DNA. The spectra were recorded at excitation wavelength 520 nm for an emission range of 550-750 nm. In the fluorescence quenching spectra, the reduction in emission intensity measures the binding propensity of complex to CT DNA. Stern-Volmer quenching constant (K_{sv}) and apparent binding constant (K_{app}) were calculated using $I_0/I=1+K_{sv}r$ and K_{EtBr} [EB]=K_{app}[Complex], where I_0 and I correspond to the fluorescence intensities of EtBr-DNA in the absence and presence of complex respectively, r is the ratio of the total concentration of complex to that of DNA, and K_{EtBr} = 1 X 10^7, [EtBr] = 4 μM and [Complex] is the concentration of the complex at 50% reduction of emission intensity of EtBr.[14]

Viscosity measurements were carried out to further clarify the binding mode of the copper(II) complexes using Brookfield Viscometer LV DV-II + Pro at 25.0 ± 0.1 °C. Viscosity values, η (Unit, cP), were measured directly by running spindle (0#) in working samples at 30 rpm via the ULA (ultra low viscosity adapter). Data are presented as η/η_0 versus [Complex]/[DNA] concentration ratio, where η_0 and η refer to the viscosity of DNA in the absence and presence of the complexes.[15]

2.4 DNA cleavage studies

The DNA cleavage experiments were performed by agarose gel electrophoresis, by incubation at 37 °C as follows: pBR322 DNA (0.1 μg/μL) in 50 mM Tris–HCl buffer (pH=7.2) was treated with copper(II) complexes containing 1% DMF. The samples were incubated for 3 h, and then loading buffer (1 μL) was added. Then the samples were subjected to electrophoresis for 3 h at 50 V on 0.8% agarose gel using Tris–Acetic acid–EDTA buffer. After electrophoresis, bands were visualized under UV light and photographed. To identify the reactive oxygen species (ROS) involved in the cleavage reaction the following scavengers like NaN_3, L-Histidine (singlet oxygen), SOD (superoxide), and DMSO (Hydroxyl) were used. The extent of cleavage of the Super coiled DNA (SC DNA) was determined by measuring the intensities of the bands using the UVITEC Gel Documentation System.[16]

2.5 Protein binding studies

Binding nature of the copper(II) complexes (**1-5)** with BSA was studied using fluorescence spectra recorded from 300 nm to 500 nm at excitation wavelength 280 nm. BSA stock solution was prepared in 50 mM phosphate buffer (PBS) (pH = 7.2) and stored in 4 ºC. All the test samples were purged with nitrogen gas for 15 min to remove dissolved oxygen. Titrations were manually carried out using micropipette by the addition of complexes. The

binding study of BSA with complexes was carried out by measuring UV spectrum in the range of 200 nm to 500 nm. Initially record the spectrum for BSA (10 μM) alone subsequently addition of the copper(II) complexes to equal molar to that of the BSA solution.

2.6 Cell line and cell culture

MCF-7 cells (Human breast cancer cells) obtained from the National Centre for Cell Science, Pune, India were used in this study. The cells were maintained in DMEM medium supplemented with 10% fetal bovine serum, 100 UmL^{-1} of penicillin and 100 μg mL^{-1} of streptomycin at 37 °C in a 5% CO_2 incubator.

2.7 Cell cytotoxicity assay (MTT assay)

MCF-7 cells grown in T25 flask (80% confluency) were used for this assay. Then, the complete medium was removed and rinsed once with 1 mL of trypsin. Then 1 mL of trypsin was added to the flask and incubated at 37 ºC for 5 min. The detached cells were suspended in complete medium and 200 μL of this cell suspension was seeded into 96 well TC plate and incubated at 37 °C for 24 h. After 24 h, the complete medium was removed and serum free medium was added and left for 4 to 6 h. Then the complex (**1**) and complex (**5**)**,** at different concentration ranges (1, 5, 10, 15, 20, 25 μM) were added in triplicate and incubated at 37 °C for 24 h. After the incubation period, 20 μL of MTT (5 mg/mL) solution was added to each well and incubated at 37 °C for 4 h in dark. Finally, the solution in each well was discarded and 100 μL of DMSO was added to each well, mixed and read at 570 nm using ELISA plate reader.

2.8 Antimicrobial activity

2.8.1 Microorganisms:

Micro organisms of gram-positive bacteria *Staphylococcus aureus* (ATCC 12600), *Bacillus subtilis* (ATCC 6633) and *Enterococcus faecalis,* gram-negative bacteria of *Proteus*

mirabilis, Pseudomonas aeruginosa, Klebsiella pneumoniae (ATCC 13883) and *Escherichia coli* (ATCC 11775) were stored in a refrigerator and used for the antimicrobial study.

2.8.2 Reference and Control:

Tetracycline was chosen as the reference compound for all bacterial species used. The control consisted of plates of solidifying agar onto which was pure solvent, and the test compounds were dissolved in it.

2.8.3 Mueller Hinton Agar (Bacteria):

Mueller Hinton Agar was purchased from HiMedia (HIMEDIA-M173-500 G) to make up the medium for bacteria. 121.6 g of Mueller Hinton Agar was suspended in 3200 mL of distilled water in a 5 L flask, stirred, boiled to dissolve and then autoclaved at 15 lbs and at 121 ºC for 15 min. The pH range was between 7.0-7.5.[17] The bacterial lawn culture was made using sterile cotton swab and labeled. The wells were made by media with the help of a metallic borer and center at least 24 mm. Recommended concentration of the test sample was introduced in the respective wells. Other wells were supplemented with reference antibacterial drug.[18] Incubation was maintained at 37 ºC for 24 h. Activity was determined by measuring the diameter of zones showing complete inhibition (mm). Growth inhibition was compared with the reference drugs.

3. Result and discussion

3.1 Synthesis and structural analysis of copper(II) complexes

New acyclic copper(II) complexes were prepared by variying the aliphatic and aromatic diamines. All the complexes were obtained in good yield; stable in air and with good solubility in DMF, DMSO, methanol, ethanol and 1% DMF/50 mM Tris-HCl buffer solution. The complexes were characterized by various spectroscopic and analytical methods. ESI-MS spectra

of the copper(II) complexes (**1-5**)(Fig. S1) showed essentially molecular ion peaks and their isotopic peak [M+1]. The crystallization of the complexes were tried in various solvents, but crystals for complex (**1**) were got only with acetonitrile solvent. The crystal structure of complex (**1**) was determined by single crystal X-ray diffraction analysis, and the selected crystallographic data of complex (**1**) are given in Table 1. FT-IR spectra of the complexes (**1-5**) displayed the peak around 1610-1636 cm^{-1} due to ν(C=N) stretching vibration, with the significant disappearance of the peak at around 1690 cm^{-1} corresponding to ν(C=O); it indicates an effective schiff's base condensation in complexes (**1-5**). The bands at ~1090 cm^{-1} and 620 cm^{-1} corresponds to ClO_4 molecule and the peak at 1090 cm^{-1} does not shows any splitting, this is in agreement with the presence of uncoordinated ionic perchlorate in their crystal lattices. All the complexes gave molar conductance value in the range of 80 – 85 S m^2 M^{-1} at 25 ºC which indicates that these complexes are 1:1 electrolyte. The electronic spectrum of complexes (**1-5)** shows a weak band around 560-630 nm, which indicates that the coordination geometry of the central metal ion might be square planar. An increase in the chain length at acyclic copper(II) complexes reveals increase in λ_{max} (red shift) value for d-d transition of copper(II) ion.

3.2 X-ray crystallographic study of acyclic mononuclear Copper (II) complex (1)

Intensity data for the complex (**1**) was collected using a Bruker AXS Kappa APEX II single crystal CCD Diffractometer equipped with graphite-monochromated MoKα radiation (λ=0.71073Å) at room temperature with a crystal dimension of 0.25 X 0.2 X 0.15 mm^3. The accurate unit cell parameters were determined from the reflections of 36 frames measured in three different crystallographic zones by the method of difference in vectors. The data collection, data reduction and absorption correction were performed by APEX2, SAINT-plus and SADABS program. The structure was solved by direct methods procedure using SHELXS-97 program and

the non-hydrogen atoms were subjected to anisotropic refinement by full-matrix least squares on F^2 using SHELXL-97 program.[12]

The ethylenediamine moiety of Cu(L1) disordered over two positions with site occupancies of 0.84(14) and 0.16(14) respectively. The perchlorate anion in the asymmetric unit also experiences an orientational disorder with site occupancies of 0.60(1) and 0.40(1) respectively. The bond distances of the disorder components were fixed using standard restraints. The atomic displacement parameters (ADP) of the minor components were allowed to move equally with the major component using suitable similarity restraints. The ADP of oxygen atoms of the disordered perchlorate anion were allowed to move isotropically. The positions of all the hydrogen atoms were identified from difference electron density map and were treated accordingly. The hydrogen atoms bound to the C atoms were allowed to ride on the parent atom with $U_{iso}(H) = 1.2U_{eq}(C)$ and $1.5U_{eq}(C)$.

The title compound crystallizes in triclinic space group P-1 with two formula units in the unit cell. The asymmetric unit of the complex (**1**) comprises one molecule of Cu(L1), one acetonitrile solvent molecule and a distorted perchlorate anion. In Cu(L1) the ethylenediamine moiety was positionally disordered over two sites and the same refined in the crystal structure. Fig. 1 shows the ORTEP representation of the compound drawn at 40% ellipsoid probability. (One of the disorder components has been removed for clarity). Table 1 gives crystal data and refinement parameters for the title compound. The Cu(II) ion has a slightly distorted square planar co-ordination with the phenolic oxygens and the nitrogens of the ethylenediamine. The displacement of the Cu(II) ion from the best plane through the donor atoms N1, N2, O1, and O2 found to be -0.0635(14) Å. The co-ordination bond angles are 89.25(11) ° (O1-Cu1-O2), 93.13(13) ° (O1-Cu1-N1), 92.74(12) ° (O2-Cu1-N2) and 84.63(2) ° (N1-Cu1-N2) respectively

and their sum being 359.75(13) ° showing the square planar coordination. Similar kind of geometry is observed in other closely relevant Cu(II) and Ni(II) structures.[19] There is a slight distortion of the coordination plane around the Cu(II) ion which can be understood from the dihedral angle between the planes N1-Cu1-N2 and O1-Cu1-O2 [5.28 (13) °]. The piperazine ring adopts chair conformation with the nitrogen atoms N3 and N4 staying in the apical position. The nitrogen atom N4 is protonated. As a result of protonation the bond distances C21-N4 [1.481 (5) Å] and C18-N4 [1.481(5) Å] are elongated compared to the unproptnated C-N bond distances.

In the crystalline solid, the assembly of molecular constituents exhibit interesting supramolecular architecture by means of C-H…O interactions. The N-H donor atom forms an intermolecular hydrogen bond with the metal coordinating oxygen atom. Table S1 shows the hydrogen bonds for complex (**1**). The centrosymmetrically related Cu(L1) molecules and the perchlorate anion are interlinked through a variety of C-H…O interaction to form a two dimensional supramolecular sheet, extending infinitely along (1 0 0) plane. This (1 0 0) sheet form an infinite three dimensional network by piling up along the a-axis stabilized by a weak C-H…..Br interaction. The supramolecular architecture forms molecular channels sufficient enough to hold the guest (solvent) molecules. In the title compound the acetonitrile solvents are getting trapped between these molecular channels and are illustrated in Fig. 2.

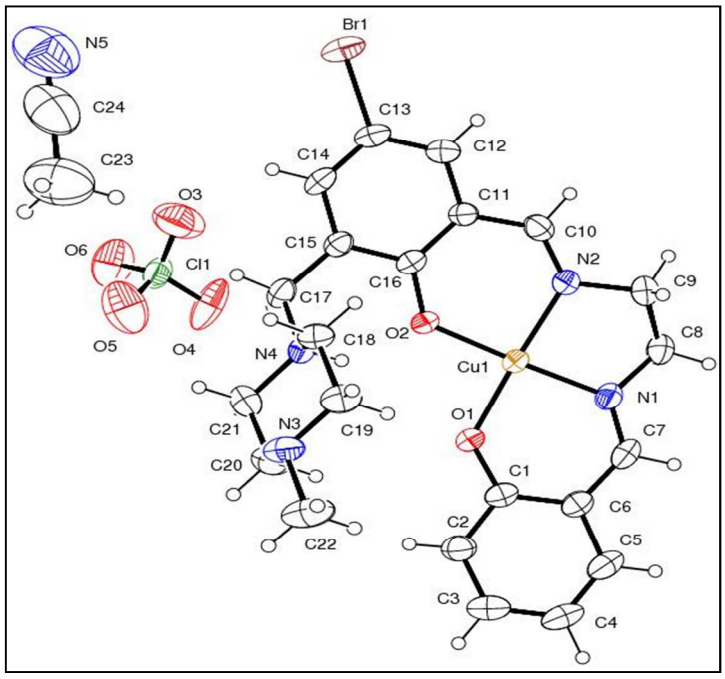

Fig. 1 ORTEP diagram representation of complex (**1**). Thermal ellipsoids are drawn at the 40% probability level.

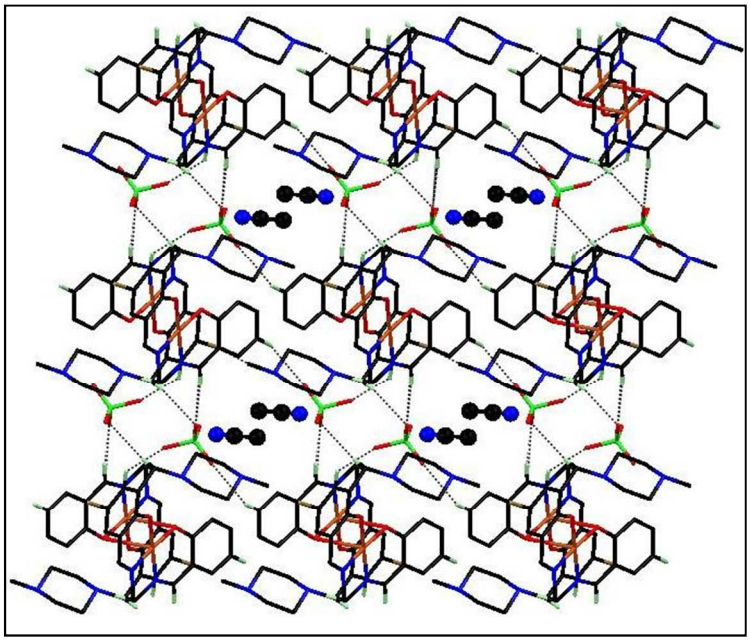

Fig. 2 Part of the crystal structure of complex (**1**) forming molecular channels through strong C-H…O interaction and a weak C-H….Br interaction [host-network represented as stick model] where the solvent molecular are trapped [solvents represented as ball & stick model]

Table 1 Crystal data and structure refinement for complex (**1**).

Empirical formula	C_{24} H_{29} Br Cl Cu N_5 O_6	
Formula weight	662.42	
Temperature	293(2) K	
Wavelength	0.71073 Aº	
Crystal system, space group	Triclinic, P-1	
Unit cell dimensions	a = 10.906(5) Aº	alpha = 102.848(5) deg.
	b = 11.079(5) Aº	beta = 113.134(5) deg.
	c = 12.921(5) Aº	gamma = 90.888(5) deg.
Volume	1390.5(10) A^3	
Z, Calculated density	2, 1.582 Mg/m^3	
Absorption coefficient	2.365 mm^{-1}	
F(000)	674	
Crystal size	0.30 x 0.20 x 0.20 mm	
Theta range for data collection	1.77º to 25.00º.	
Limiting indices	-12<=h<=12, -13<=k<=13, -10<=l<=15	
Reflections collected / unique	21175 / 4841 [R(int) = 0.0502]	
Completeness to theta = 23.15	98.9%	
Max. and min. transmission	0.6491 and 0.5372	
Refinement method	Full-matrix least-squares on F^2	
Data / restraints / parameters	4841 / 87 / 403	
Goodness-of-fit on F^2	1.001	
Final R indices [I>2sigma(I)]	R1 = 0.0372, wR2 = 0.0873	
R indices (all data)	R1 = 0.0670, wR2 = 0.1028	
Largest diff. peak and hole	0.582 and -0.319 $e.A^{-3}$	

3.3 Electrochemical characterization

Electrochemical properties of the complexes (**1-5**) were studied by cyclic voltammetry in the potential range from -0.6 to -1.4 V containing 0.1 M TBAP and the data are summarized in Table 2. The cyclic voltammograms of the acyclic copper(II) complexes are shown in Fig. 3. Cyclic voltammetric response of complexes (**1-5**) at negative potential may be attributed to the presence of electronegativity and hard nature of the phenoxide group present in the complexes.[20] Herein, all complexes show one quasireversible reduction wave at negative potential in the range from -0.93 to -1.13 V. Typically, quasi reversible nature of the metal complexes satisfy the following conditions. (i). The E_{pc} and E_{pa} values change with increase in scan rate (ii). ΔE_p values increases with increasing the scan rate and are greater than 60 mV (iii). Cathodic peak currents (I_{pc}) are greater than the anodic peak currents (I_{pa}). All the copper(II) complexes (**1-5**) satisfied the above conditions, strongly suggesting that copper(II) ion in these complexes reduced to Cu(I) ion and the redox process is quasi reversible in nature. The cyclic voltamogramm shows that the reduction potential of the copper(II) complexes are shifted towards anodic region when the chain length of the diamines increases. For example the complex (**1**) has E^1_{pc} = -1.13 V, which is more negative compare to complex (**2**) E^1_{pc} = -0.96 V, the same observation was inferred for the aromatic amine based complexes **(3-5)**. The ΔE values of all the complexes gradually decreased with increasing the chain length of the diamines in copper(II) complexes (**1-5**). The above observation may be due to the whole system becomes more flexible and hence undergoes easy reduction with increasing chelate ring size.[21]

.

Table 2 Electrochemical data of copper(II) complexes (**1**-**5**)

Complexes	E_{pc}/V	E_{pa}/V	$E_{1/2}$/V	ΔE/mV
1	-1.13	-1.00	-1.07	130
2	-0.96	-0.84	-0.90	120
3	-1.06	-0.97	-1.02	90
4	-0.96	-0.88	-0.92	80
5	-0.93	-0.85	-0.89	80

Measured by Clyclic voltammograms at 100 mV/s conditions: GCE working; Ag/AgCl reference electrodes and TBAP as a supporting electrolyte; [Complex] = 1 X 10^{-3} M; [TBAP] = 0.1 M.

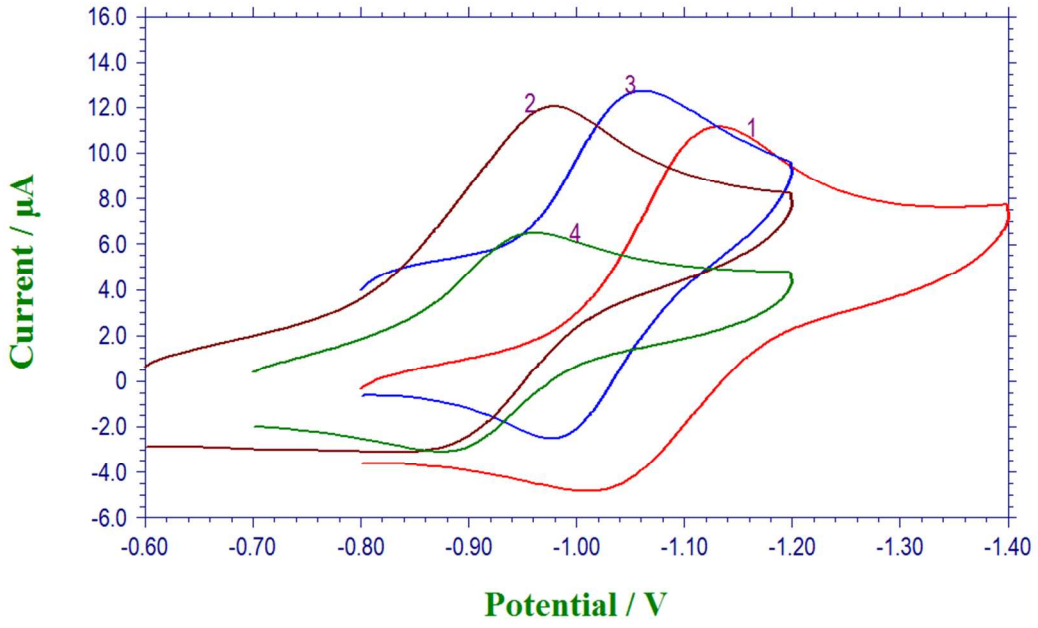

Fig 3. Cyclic voltammogram of copper(II) complexes (**1**), (**2**), (**3**), and (**4**).

3.4 DNA binding studies

3.4.1 Absorption spectroscopic studies

Electronic absorption spectroscopy is usually employed to examine the binding ability of metal complexes with DNA helix. The synthesized copper(II) complexes are bound to DNA through intercalation and it is characterized by a change in absorbance as well as bathochromic shift in wavelength and the extent of hypochromism. The intercalative mode involving a strong stacking interaction between the aromatic chromophore moieties of the copper(II) complexes and DNA base pairs.[22] The extent of hypochromism is commonly a measure of the strength of intercalative interaction[23]. Fig. 4 shows the absorption spectra of complex (**1**) after addition of CT DNA and Fig. S2 shows the same for complex (**4**) and complex (**5**). The addition of CT DNA to complexes (**1**), (**4**) and (**5**) shows that the decrease in absorbance of the π-π* band and metal to ligand charge transfer (MLCT) band. It indicates that the binding of the complexes with DNA are very strong. The binding strength of copper(II) complexes (**1**), (**4**) and (**5**) with CT DNA are 8.4 X 10^3, 1.9 X 10^4 and 3.0 X 10^4 M^{-1}, respectively. p-Bromo substituted copper(II) complexes have higher DNA binding constant values than the p-methyl substituted copper(II) complexes.[6,14] The higher binding constant may be due to larger electro-negativity and less space hindrance of bromo than the methyl group and also due to the fact that the binding activities depend on the charge of the molecule, electron density present in the donor site, number of potential binding sites available to bind DNA[23d]. The synthesized copper(II) complexes contain biologically active piperazine group with potential N donor binding sites. The lone pair electron present in the piperazine group may interact with DNA molecule. This interaction may alter binding constant and cleavage activity of the complexes.

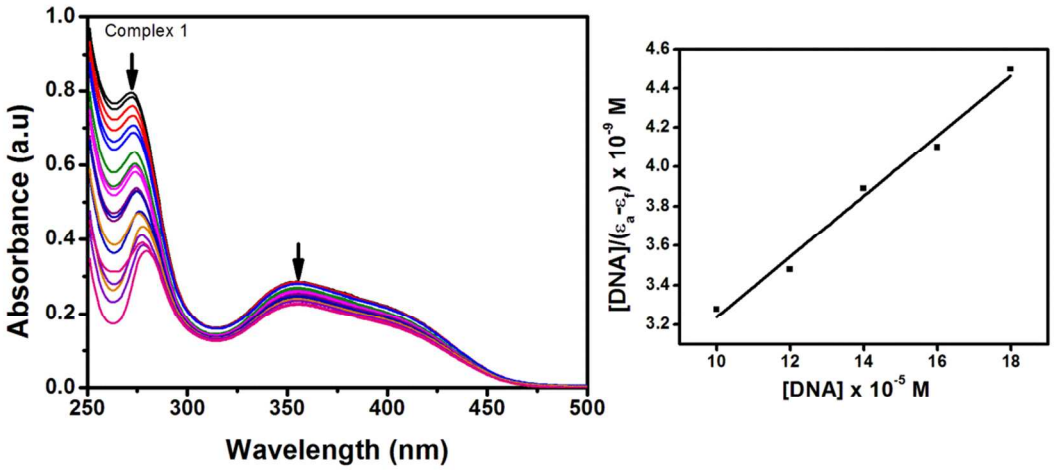

Fig. 4 Absorption spectra of the complex (**1**) in the absence and presence of increasing amounts of CT-DNA (0 – 250 µM) at 25 ºC in 50 mM Tris-HCl (pH = 7.2).

The binding constant (K_b) values of the copper(II) complexes occur in the order (**5**) > (**4**) > (**1**), and these complexes show good hypochromism (52% for complex **1**; 36% for complex **4** and 51% for complex **5**) as well as small red shift. The binding constant (K_b) values of the complexes were found to be lower than typical classical intercalates EtBr[24] (K_b = 3.38 X 10^5 M^{-1}). The magnitude of these binding constant values clearly showed that the complexes bind with CT DNA through intercalation. The complex (**5**) binds more strongly than the complex (**1**) and (**4**) and this may be due to more surface area of aromatic (napthalene) moiety present in complex (**5**) which enhances the extent of binding with DNA base pairs.[25]

3.4.2 Competitive binding studies between EB and copper(II) complexes for CT-DNA

In order to confirm the intercalative mode of binding between copper(II) complexes and CT-DNA, an ethidium bromide (EtBr) fluorescence displacement experiment was also carried out. It has been previously reported that the fluorescence intensity of EtBr-DNA system is quenched by adding certain complexes. This indicate that the complexes is bound to the base pairs of DNA by intercalation mode while replacing the EtBr.[26]

The fluorescence quenching spectrum of DNA-bound EtBr by complex (**5**) is shown in Fig. 5 while the spectra for complexes (**1**) and (**4**) are in (Fig. S3). The fluorescence quenching spectra show that the addition of the complexes to DNA-bound EtBr, the emission band at 615 nm exhibited hypochromism, up to 46%, 53% and 61% of the initial fluorescence intensity accompanied by small red shift of 2 nm, 2 nm and 3 nm for complexes (**1**), (**4**) and (**5**), respectively. The hypochromism and red shift indicate that EtBr molecules are replaced from DNA-bound EtBr system by the complexes. There are two mechanisms proposed for the quenching of DNA-bound EtBr by complexes, one is replacement of molecular fluorophores and another one is electron transfer.[27]

The classical Stern-Volmer quenching constant was calculated by the following equations: $I_o/I = 1+K_{sv}r$, where I and I_o are fluorescence intensity in the presence and absence of CT-DNA, respectively and r is the ratio of total concentration of the complex to that of DNA [Complex]/[DNA]. From the plot of I_o/I versus [complex]/[DNA], the linear Stern-Volmer quenching constant K_{SV} can be calculated from the ratio of slope to intercept. The K_{SV} values for the complexes (**1**), (**4**) and (**5**) are 0.64 (R = 0.966), 0.89 (R = 0.994) and 1.14 (R = 0.974) respectively.

Further, the apparent binding constant (K_{app}) values were obtained for the compounds using the following Eq (2):[28]

$$K_{EtBr} \text{ X } [EtBr] = K_{app} \text{ X } [complex] \qquad (2)$$

where, the concentrations of the complexes were taken for observing a 50% reduction of the emission intensity of EtBr. The DNA binding constant value is 1.0 X 10^7 M^{-1} for EtBr.[29] Apparent DNA binding constants values were found to be 1.9 X 10^6 M^{-1}, 3.29 X 10^6 $M^{-1}$and 4.2 X 10^6 M^{-1} for complexes (**1**)**,** (**4**) and (**5**), respectively. The quenching

constants and binding constants values suggest that the interaction of complexes with DNA should be intercalation. Further, since hydrophobic environment inside the DNA double helix reduces the accessibility of solvent water molecules to the complex, the complex's mobility is simply restricted at the binding sites so that complexes can strongly interact with DNA and are protected by DNA efficiently.

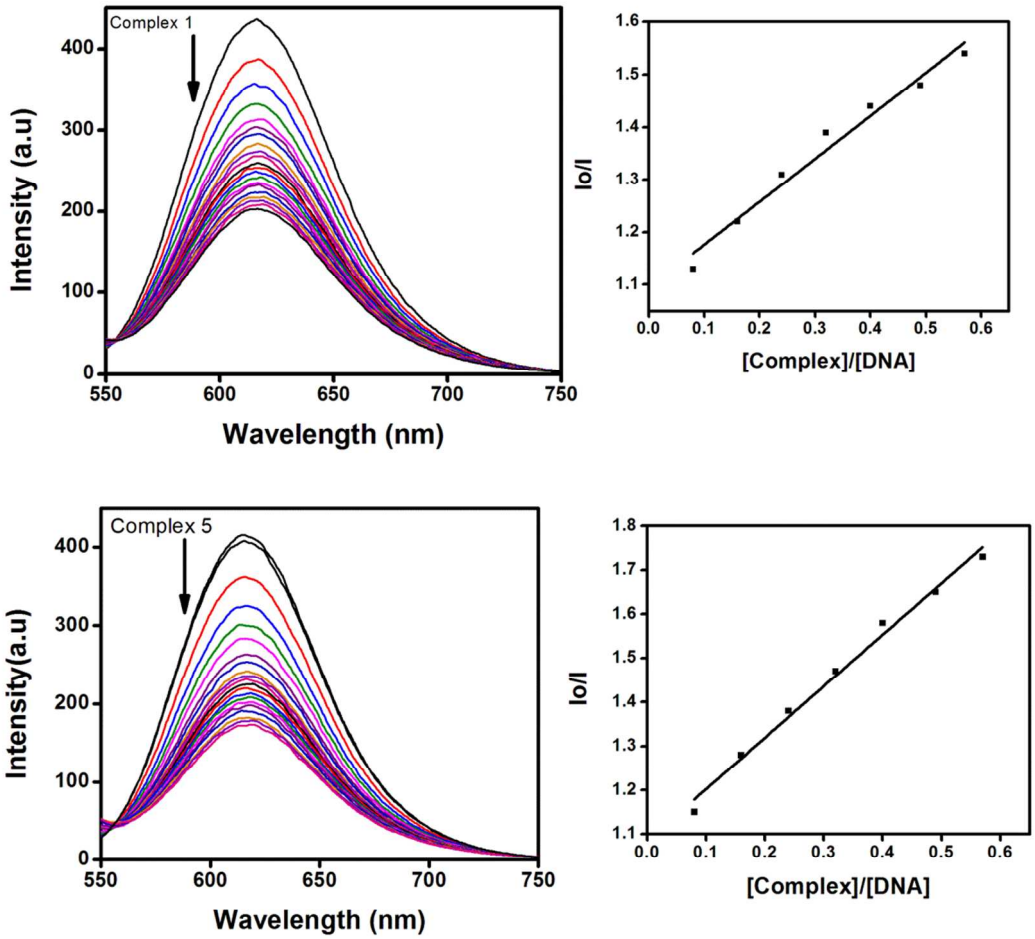

Fig. 5 Emission spectra (λ_{ex} = 520 nm) of EB-DNA in Tris-HCl buffer in the absence and presence of the Complex (**1**) (a) and (**5**) (b). [EtBr] = 4 μM, [DNA] = 40 μM. Arrow shows the decrease on intensity of EtBr-DNA upon increasing the concentration of complex.

3.4.3 Viscosity studies

The interaction of complexes with CT DNA was also evaluated by viscosity measurements in solution and it gives further evidence for an intercalative binding mode. The

viscosity of DNA solution increases due to partial and/or complete intercalation of complexes in-between the DNA base stacks, which reduce electrostatic/covalent interactions within DNA. The relative specific viscosities of DNA were investigated after addition of the complexes. Upon increasing the concentration of copper(II) complexes, the relative viscosity of DNA simultaneously increases (Fig. 6). It is due to the aromatic chromophore of the complexes intercalates with CT DNA base pairs and increase the length of CT DNA. Fig. 6 and Fig. S4 clearly show that the order of increasing viscosity of the CT DNA solution (**5**) > (**4**) > (**3**) > (**2**) > (**1**)**.** The above results match the classical intercalating molecule like EtBr binding with DNA. The increase in the length of DNA molecule upon insertion of the EtBr between the base pairs of DNA and increases the DNA viscosity.[30] However the lower binding constant of the reported complex (1), as for a similar compound reported by Sato *et al.,*[30a] favors groove binding mode. By considering both the facts the complex (1) may probably bind with DNA partly through partly through intercalative and partly through groove binding modes.

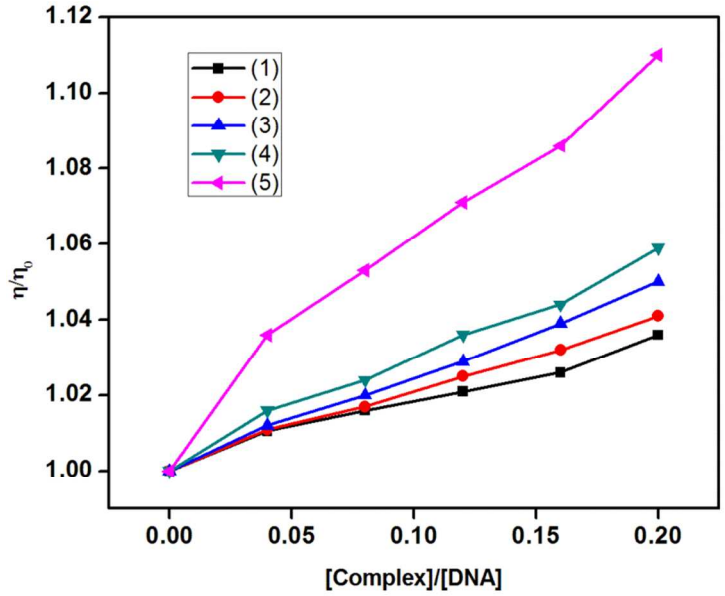

Fig. 6 Relative viscosity shows the effect of increasing the concentration of complexes (**1**), (**4**) and (**5**) to CT-DNA at 25 ºC. [DNA] = 0.5 mM and [complex]/[DNA] = 0.00, 0.04, 0.08, 0.12, 0.16, 0.2 respctively.

3.4.4 CD spectral studies

The conformational changes of CT-DNA induced by complexes (**1**) and (**5**) were monitored by CD spectroscopy in Tris-HCl buffer medium at 25 ºC as shown in Fig.7. The UV CD spectrum of CT DNA consists of a positive band at 275 nm, which is due to base stacking and negative band at 245 nm due to B-DNA.[31] On incubation with complexes (**1**) and (**5**) to the solution of CT DNA, the CD band intensities decrease for the positive band and increase for the negative band. The maximum decrease in intensity of the DNA helicity band with a higher red-shift observed for complex (**5**) which indicates that this complex exhibits a mode of DNA binding different from complex (**1**). It is may be due to the presence of naphthalene ring in complex (**5**), enhancing the maximum interaction. The interaction with cations effectively screens the negative charge on N(7) base sites as well as phosphate oxygens simultaneously, both from deoxyribophosphate back-bone and in the groove of the helix, to promote such a transconformational change. The decrease in positive band and increase in the negative band indicate strong conformational changes.

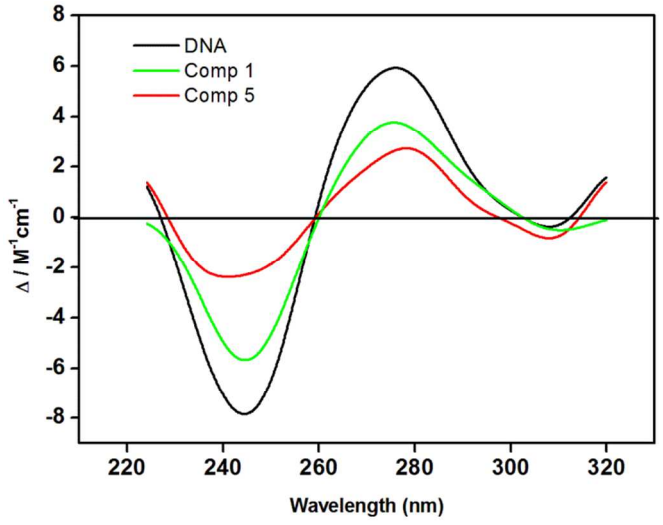

Fig. 7 CD spectra of CT-DNA (100 μM) in the absence and the presence of complexes (**1**) and (**5**) (10 μM).

3.5 DNA cleavage studies:

The DNA cleavage activities of copper(II) complexes (**1**), (**4**) and (**5**) (Fig. 8) same for complex (**3**) is given in (Fig. S4) were investigated toward supercoiled pBR322 mM plasmid DNA (50 μg mL^{-1}) and 50 mM Tris-HCl buffer (pH = 7.2) in presence of 1 mM mercaptoethanol as a reducing agent and the reaction mixture was incubated at 37 ºC for 1h. Agarose gel electrophoresis was used to monitor the conversion of supercoiled pBR322 DNA (SC DNA) to the nicked circular (NC DNA) and linear open circular DNA (LC DNA).[32] The control experiments suggest that untreated DNA and DNA incubated with $Cu(ClO_4)_2.6H_2O$ did not show any notable DNA cleavage (Lane 1 and Lane 2; Fig. 8). The pictures of the complexes (30 μM) show that the order of cleavage is as (**5**) > (**4**) > (**3**) > (**1**). The graphical representation (Fig. 8 A) shows the cleavage efficiency of copper(II) complexes; the complex (**5**) forms maximum amount of LC DNA. Hence the formation of LC DNA increased with increasing the aromatic moiety of the copper(II) complexes.

The mechanistic aspects of the chemical nuclease activities were investigated with various quenchers. The addition of singlet oxygen quenchers like L-hisditine, NaN_3 (Lane 4 and Lane 5) shows significant inhibition of the DNA cleavage process, it exhibited that the possibility of the singlet oxygen as the reactive species involved in the cleavage process.[33] Moreover, with the addition of hydroxyl radical scavengers such as DMSO, KI (Lane 6 and Lane 7), there is no inhibition observed in the DNA cleavage, which indicated that the hydroxyl radical is not involved in the cleavage process. Upon addition of superoxide dismutase (Lane 8) to the reaction mixture no inhibition in the DNA cleavage was observed and this revealed that the superoxide anion is not involved in the DNA cleavage process.

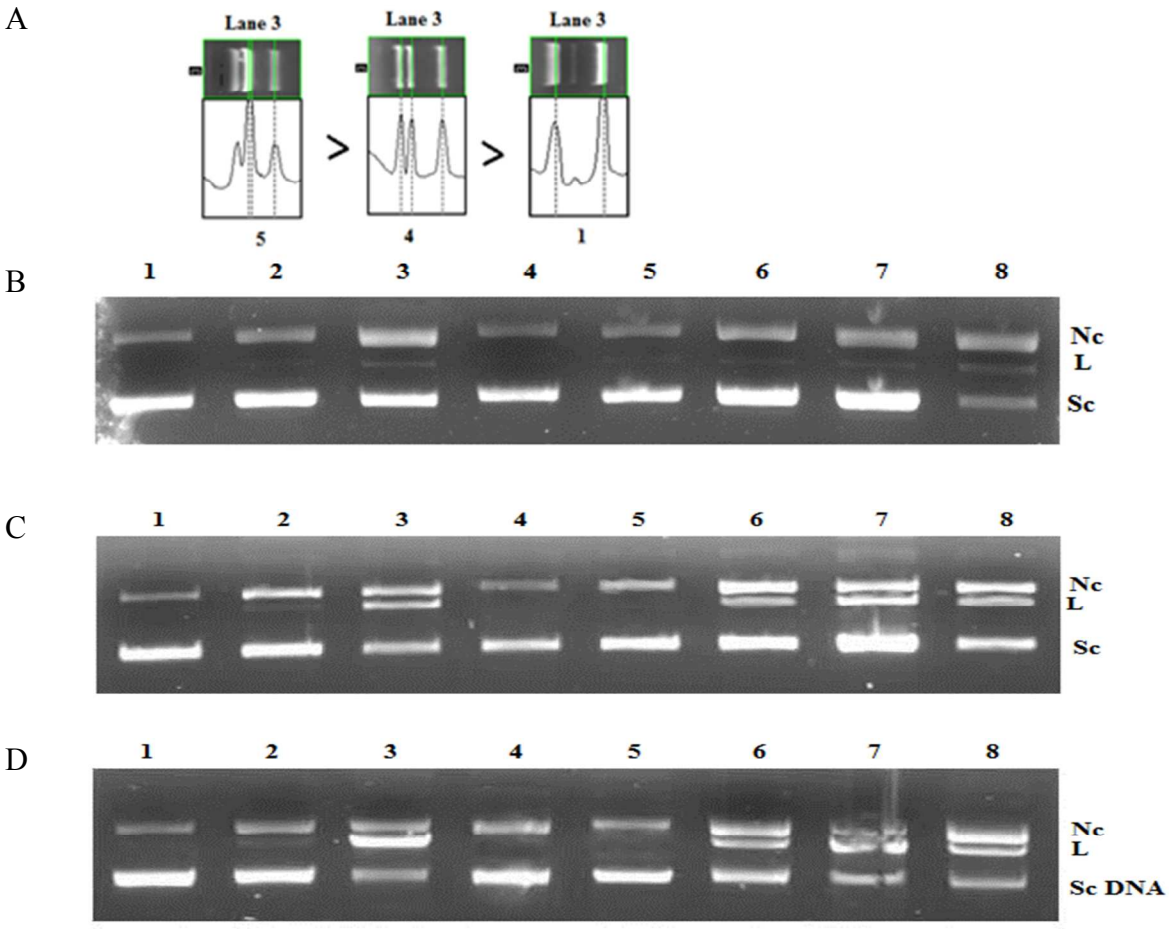

Fig. 8 Gel electrophoresis diagrams shows the cleavage of supercoiled pBR322 DNA (150 μg mL^{-1}) by copper(II) complexes (**1**), (**4**) and (**5**) (0.03 mM) in presence of mercaptoethanol(ME) (1 mM) as reducing agent in (50 mM)Tris-HCl buffer at pH 7.2 and 37 °C with an incubation time of 3 h and different quenchers. (A) Graphical representation of cleavage efficiency of mononuclear copper(II) complexes (**1**), (**4**), (**5**). (B) Lane 1, DNA control; Lane 2, DNA + ME + $Cu(ClO_4)_2.6H_2O$; Lane 3, DNA + ME + (**1**); Lane 4, DNA + ME + (**1**) + NaN_3 (2 μL); Lane 5, DNA + ME + (**1**) + $_L$-histidine (1 mM); Lane 6, DNA + ME + (**1**) + DMSO (1 mM); Lane 7, DNA + ME + (**1**) + KI; Lane 8, DNA + ME + (**1**) + SOD (5 units); (C) Lane 1, DNA control; Lane 2, DNA + ME + $Cu(ClO_4)_2.6H_2O$; Lane 3, DNA + ME + (**4**); Lane 4, DNA + ME + (**4**) + NaN_3 (2 μL); Lane 5, DNA + ME + (**4**) + $_L$-histidine (1 mM); ; Lane 6, DNA + ME + (**4**) + DMSO (1 mM); Lane 7, DNA + ME + (**4**) + KI; Lane 8, DNA + ME + (**1**) + SOD (5 units); (D) Lane 1, DNA control; Lane 2, DNA + ME + $Cu(ClO_4)_2.6H_2O$; Lane 3, DNA + ME + (**5**); Lane 4, DNA + ME + (**5**) + NaN_3 (2 μL); Lane 5, DNA + ME + (**5**) + $_L$-histidine (1 mM); Lane 6, DNA + ME + (**5**) + DMSO; Lane 7, DNA + ME + (**5**) + KI; Lane 8, DNA + ME + (**1**) + SOD (5 units).

3.6 Protein binding studies

3.6.1 UV-vis absorption studies.

Two types of quenching mechanism can occur, such as dynamic and static quenching. In the dynamic quenching mechanism, only the excited state fluorescence molecule undergoes change in the absorption spectra. In the static quenching mechanism, complex formation between quencher and fluorophore molecule occurs in ground state, thus considerably changing the absorption in UV-vis spectra. Fig. 9 shows change in absorption spectra of BSA and BSA-complex. The absorption spectra of BSA occurred at 278 nm, while addition complexes, the absorption decreased with small red shift. This result revealed that the mechanism of static quenching interaction between BSA and copper(II) complexes operates due to the formation of new ground state complexes of the type BSA-complex.[34]

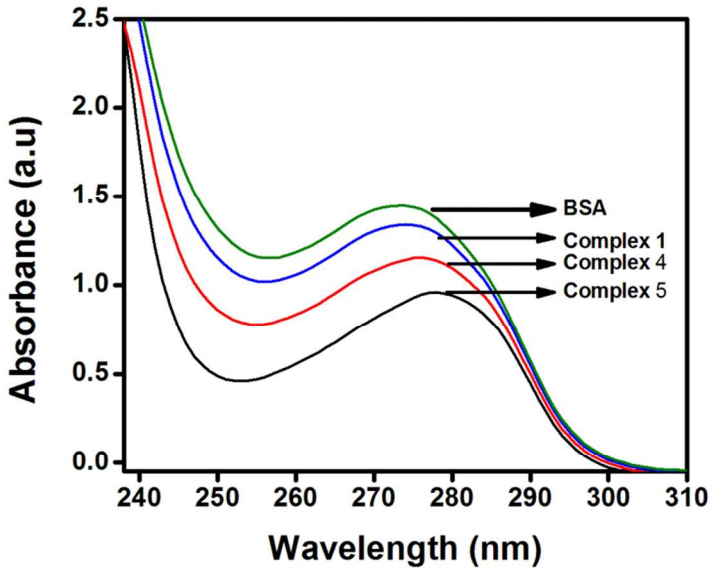

Fig 9. UV-vis absorption spectrum of BSA absence and presence of copper(II) complexes (**1**, **4** and **5**). [BSA] = [Complex] = 10 μM.

3.6.2 Fluorescence quenching studies

Fluorescence quenching study was performed for understanding the interaction of complexes with BSA. Fluorescence quenching studies show decrease in the fluorescence intensity from a fluorophore. It occurs by different types of mechanism, such as ground state complex formation, excited state reaction, energy transfer and collision quenching. On the addition of complexes to the solution BSA shows decrease in fluorescent intensity with small red shift as in Fig. 8 complex (**1**) Fig. S5 shows same for the complexes (**2**), (**3**), (**4**) and (**5**). It is due to the active site in BSA being buried in a hydrophobic environment which means that the complexes interact with blood carrier protein.[35]

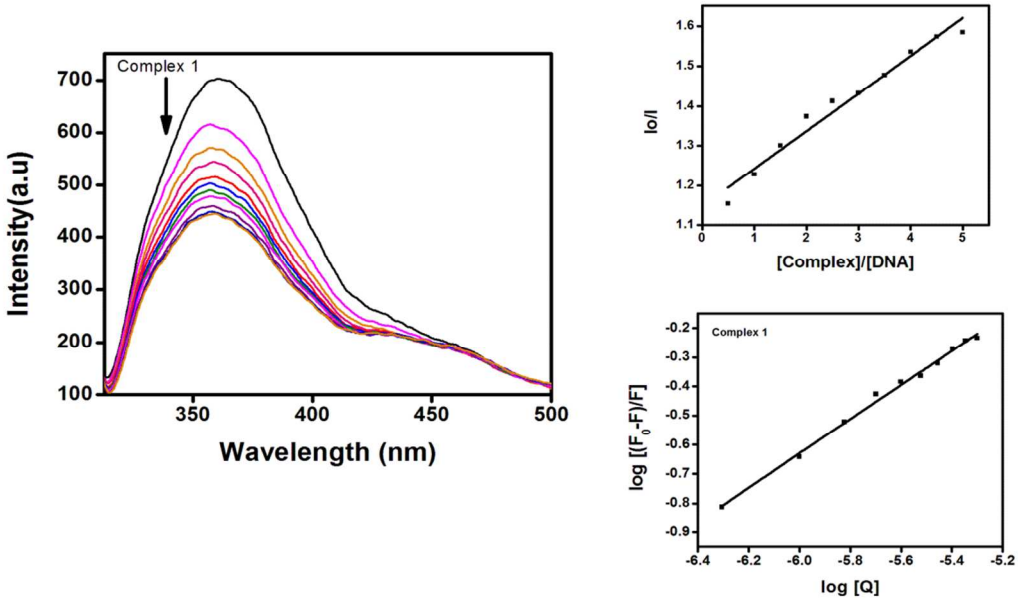

Fig. 10 Changes in the fluorescence spectra of BSA upon increasing complex (**1**) concentration at 300 K. The concentration of BSA is 1 μM and complex concentration range from 0.0 to 10 μM, pH = 7.2 and λex = 280 nm.

The fluorescence quenching can be described by Stern-Volmer relation :

$$I_0 / I = 1 + K_{SV}[Q] \quad (3)$$

where I_0 and I are the fluorescence intensities of the fluorophore in the absence and presence of quencher respectively, Ksv is the Stern-Volmer quenching constant and [Q] is the quencher concentration.

The small molecules bind independently with set of equivalent sites of macromolecule, the binding constant (K_b) and the number of binding sites (n) can be determined by the following Eq[4]:[36]

$$\log [(F_0 - F)/F] = \log K_b + n \log [Q] \quad (4)$$

where in the present case, F_0 and F are the fluorescence intensities in the absence and presence of quencher respectively, [Q] is the concentration of quencher and K_b is the binding constant for the complex-protein interaction and n is the number of binding sites per albumin molecule, which can be determined by the slope and the intercept of the double logarithmic plot of log $[(F_0\text{-}F)/F]$ vs log[Q] based on equation (4). The calculated value of Stern-Volmer quenching constant (K_{SV}), binding constant (K_{bin}), and the number of binding sites (n) are listed in Table 3. The values of n are approximately equal to 1, indicating a single binding site in BSA for all the complexes. The values of K_{bin} indicate a strong interaction between the copper(II) complexes and BSA. The binding constant values indicate that the complex (**5**) shows stronger binding to BSA than the other complexes. The complex (**5**) possess a naphthalene group and this may interact with the active site.

Table 3 Static binding constants (K_{bin} in M^{-1}) and binding sites for the interaction of copper(II) complexes (**1**-**5**) with BSA at 298 K.

Complexes	**K_{sv} (mol L^{-1})**	**Quenching rate constant K_q ($M^{-1}s^{-1}$)**	**K_{bin} (L mol^{-1})**	**The number of binding sites per BSA n**
1	8.2 X 10^4	8.2 X 10^{12}	0.772 X 10^3	0.586
2	6.9 X 10^4	6.9 X 10^{12}	0.294 X 10^4	0.725
3	8.4 X 10^4	8.4 X 10^{12}	0.43 X 10^5	0.96
4	2.2 X 10^5	2.2 X 10^{13}	0.584 X 10^5	0.86
5	1.25 X 10^5	1.25 X 10^{13}	0.785 X 10^5	0.969

3.7 Cell cytotoxicity assay (MTT assay)

A common limitation of the use of new pharmaceutical compounds is their cytotoxicity,[37] which prompted us to evaluate the cytotoxic effect of copper(II) complexes in MCF-7 cells using the MTT test. MCF-7 cells were treated with crystallized complex (**1**) and complex (**5**) at various concentrations (1, 5, 10, 15, 20, 25 μM, diluted in DMEM medium) for 24 h and the cytotoxicity induced by complex (**1**) and complex (**5**) were examined. The MTT assay result is presented in Fig. 11, from the MTT assay results, complex (**1**) and complex (**5**) exhibited significant cytotoxicity in MCF-7 cells in a concentration-dependent manner. IC_{50} value for complex (**1**) is 4.212 μM and for complex (**5**), it is less than 1 μM which confirmed that complex (**5**) has considerably higher cell growth inhibition than the complex (**1**) against the MCF-7 cells.

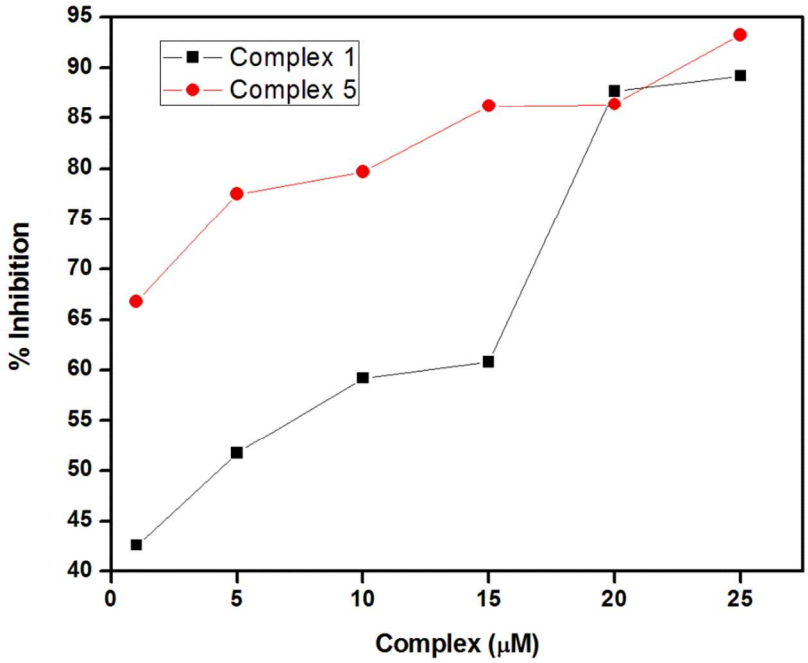

Fig. 11 Effect of complex (**1**) on cell viability of MCF-7 cells. The values are mean ± SD of 3 experiments.

3.8 Antimicrobial activity

The complex (**1**) and complex (**5**) (Table S2) showed the maximum zone of inhibition against *Enterococcus faecalis* and *Pseudomonas aeruginosa* at 100 μg mL^{-1} concentration. Both the complexes showed zones of inhibition for all the 7 microorganisms (Fig, 12 and Fig S6) with values ranging from 50, 75 and 100 μg mL^{-1} concentrations showed in Table 4 and Table S2.[38] This specificity of activity may be due to the sensitivity of the test compounds associated with the different cell wall structures of bacteria, while the cell walls of bacteria contain murein.[39] In addition, the antibacterial activity of complex (**1**) and complex (**5**) probably is associated to cell capsular degradation and cell wall synthesis inhibition.[40]

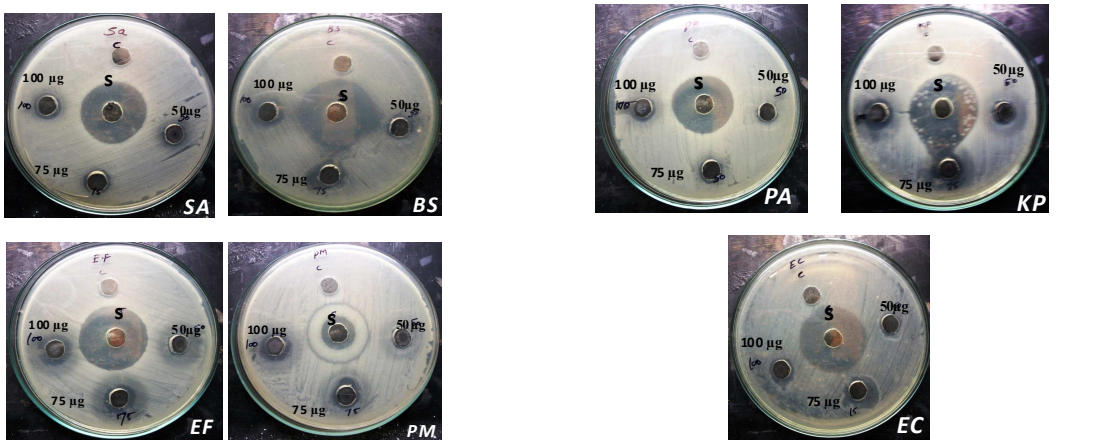

Fig. 12 Antimicrobial activity of complex (**1**) against S. aureus, B.subtilis, E. faecalis, P. mirabilis, P. aeruginosa, K. pneumoniae and E. coli.

Table 4 Antimicrobial activity of complex (**1**)

	Organisms	Concentration		
		50 µg	75 µg	100 µg
		Zone of inhibition, mm		
(**1**)	*Staphylococcus aureus*	12	14	16
	Bacillus subtilis	12	14	18
	Enterococcus faecalis	12	16	18
	Proteus mirabilis	-	12	16
	Pseudomonas aeruginosa	-	12	14
	Klebsiellapneumonia	12	15	16
	Escherichia coli	12	16	16

3.9 Conclusion

A series of multidentate copper(II) complexes are synthesized and characterized for their DNA/BSA binding, DNA cleavage, cytotoxic properties and antimicrobial activities. The binding constant (K_b) values of the complexes (**1**) and (**5**) are 0.84 X 10^4(**1**), and 3.0 X 10^4 M^{-1}(**5**) are calculated using absorption spectroscopic method and apparent binding constant (K_{app}) are calculated as 1.9 X 10^6 M^{-1}(**1**) and 4.2 X 10^6 M^{-1} (**5**) by fluorescence spectroscopy. The higher binding properties of complex (**5**) confirmed that the presence of naphthalene moiety in the acyclic ring leads to maximum intercalative interaction compare to aliphatic (ethylene) moiety. The cleavage efficiency of complexes with pBR322 DNA follows the order (**5**) > (**4**) > (**3**) > (**1**). The copper(II) complex (**5**) showed higher cleavage activity than the other complexes may be due to the presence of naphthalene group in the complex. The mechanistic investigation confirms

that the singlet oxygen involved in the cleavage process. Results from absorption and fluorescence spectroscopic experiments suggests that all the copper(II) complexes (**1**-**5**) could interact high affinity during binding with BSA and quench the fluorescence of BSA through a static mechanism. According to the present work a good overall correlation exists between DNA/BSA binding and DNA cleavage activity for the complex (**5**). Thus complex (**5**) is a promising candidate for further studies.

Appendix A. Supplementary data

CCDC 978676 contains the supplementary crystallographic data for complex (**1**). These data can be obtained free of charge via http://www.ccdc.cam.ac.uk/conts/retrieving.html,or from the Cambridge Crystallographic Data Centre, 12 Union Road, Cambridge CB2 1EZ, UK; fax: (+44) 1223-336-033; or e-mail: deposit@ccdc.cam.ac.uk.

Acknowledgments

We gratefully acknowledge the financial support from Department of Science & Technology (DST), Government of India. One of the Authors E. Sundaravadivel thanks to Dr. C. Sivaraj, Department of CAS Botany, University of Madras, for guidance in antimicrobial studies.

References

1. (a) Y. Iwasaki, M. Kimura, A. Yamada, Y. Mutoh, M. Tateishi, H. Arii, Y. Kitamura, M. Chikira, *Inorg. Chem. Commun*., 2011, **14**, 1461–1464; (b) A. D. Tiwari, A. K. Mishra, S. B. Mishra, B. B. Mamba, B. Maji, S. Bhattacharya, *Spectrochim. Acta, Part A*., 2011, **79**, 1050–1056; (c) B. L. Fei, W. Li, W. S. Xu, Y. G. Li, J. Y. Long, K. Z. Shao, Z. M. Su, W. Y. Sun, Q. B. Liu, *J. Photochem. Photobiol. B*., 2013, **125**, 32–41.
2. (a) D. S. Raja, N. S. P. Bhuvanesh, K. Natarajan, *Inorg. Chem*., 2011, **50**, 12852-12866; (b) T. Boulikas, M. Vougiouka, *Oncol. Rep.*, 2003, **10**, 1663-1682; (c) D. Wang, S. Lippard, *J. Nat.*

Rev. Drug Discovery., 2005, **4**, 307-320; (d) M. Galanski, V. B. Arion, M. A. Jakupec, B. K. Keppler, *Curr.Pharm. Des.,* 2003, **9**, 2078-2089; (e) A. M. Angeles-Boza, P. M. Bradley, P. K. L. Fu, S. E. Wicke, J. Bacsa, K. M. Dunbar, C. Turro, *Inorg. Chem.,* 2004, **43**, 8510-8519.

3. (a) P. Krishnamoorthy, P. Sathyadevi, A. H. Cowley, R. R. Butorac, N. Dharmaraj, *Eur. J. Med. Chem.,* 2011, **46**, 3376-3387; (b) M. F. Primik, S. Goschl, M. A. Jakupec, A. Roller, B. K. Keppler, V. B. Arion, *Inorg. Chem.,* 2011, **49**, 11084-11095; (c) V. Rajendiran, K. Karthik, M. Palaniandavar, H. Stockli-Evans, V. S. Periasamy, M. A. Akbarsha, B. S. Srinag, H. Krishnamurthy, *Inorg. Chem.*, 2007, **46**, 8208-8221; (d) K. Ghosh, P. Kumar, N. Tyagi, U. P. Singh, N. Goel, A. Chakraborty, P. Roy, M. C. Baratto, *Polyhedron*., 2011, **30**, 2667–2677.

4. (a) S. S. Bhat, A. A. Kumbhar, H. Heptullah, A. A. Khan, V. V. Gobre, S. P. Gejji, V. G. Puranik, *Inorg. Chem*., 2011, **50**, 12852-12866; (b) T. Miura, A. Hori-i, H. Mototani, H. Takeuchi, *Biochemistry*., 1999, **38**, 11560–11569; (c) B. C. Bales, T. Kodama, Y. N. Weledji, M. Pitie, B. Meunier, M. M. Greenberg, *Nucleic Acid Res.*, 2005, **33**, 5371–5379.

5. C. P. Meher, A. M. Rao, M. Omar, *AJPSR.,* 2013, **3**, 43-60

6. E. Sundaravadivel, M. Kandaswamy, B. Varghese, *Polyhedron*., 2013, **61**, 33–44.

7. (a) Z. Ma, F. E. Jacobsen, D. P. Giedroc, *Chem. Rev*., 2009, **109**, 4644-4681; (b) A. Atkinson, D. R. Winge, *Chem. Rev*., 2009, **109**, 4708-4721; (c) H. Liu, X. Shi, M. Xu, Z. Li, L. Huang, D. Bai, Z. Z. Zeng, *Eur. J. Med. Chem*., 2011, **46**, 1638-1647

8. (a) T. Peter, *Adv. Protein Chem.*, 1985, **37**, 161–245; (b) J. Toneatto, G. A. Arguello, *J. Inorg. Biochem*., 2011, **105**, 645–651; (c) R. T. A. McGillivray, D. W. Chung, E. W. Davie, *Eur. J. Biochem*., 1979, **98**, 477-485.

9. (a) B. P. Esposito, R. Najjar, *Coord. Chem. Rev.,* 2002, **232**, 137-149; (b) D. S. Raja, N. S. P. Bhuvanesh, K. Natarajan, *Inorg. Chem*., 2011, **50**, 12852-12866

10. (a) J. Reim, B. Krebs, *J. Chem. Soc., Dalton Trans*., 1997, 3793–3804; (b) L. Rigamonti,

F. Demartin, A. Forni, S. Righetto, A. Pasini, *Inorg. Chem*., 2006, **45**, 10976-10989; (c) J. P. Costes, F. Dahan, M. B. F. Fernandez, M. I. F. Garcia, A. M. G. Deibe, J. Sanmartin, *Inorg. Chim. Acta*., 1998, **274**, 73-81.

11. M. Thirumavalavan, P. Akilan, M. Kandaswamy, *Inorg. Chem*., 2003, **42**, 3308-3317.

12. G. M. Sheldrick, *Acta Crystallogr. Sect. A.,* 2008, **64**, 112-122.

13. P. R. Reddy, A. Shilpa, N. Raju, P. Raghavaiah, *J. Inorg. Biochem*., 2011, **105**, 1603-1612.

14. (a) S. Anbu, M. Kandaswamy, B. Varghese, *Dalton Trans*., 2010, **39**, 3823 – 3832; (b) S. Anbu, S. Shanmugaraju, M. Kandaswamy, *RSC Advances*., 2012, **2**, 5349 – 5357; (c) S. Anbu, M. Kandaswamy, P. Suthakaran, V. Murugan, B. Varghese, *J. Inorg. Biochem*., 2009, **103**, 401 – 410; (d) L. Leelavathy, S. Anbu, M. Kandaswamy, N. Karthikeyan, *Polyhedron*., 2009, **28**, 903 – 910; (e) S. Anbu, M. Kandaswamy, P. S. Moorthy, M. Balasubramanian, M.N. Ponnuswamy, *Polyhedron*., 2009, **28**, 49 -56; (f) S. Anbu, M. Kandaswamy, *Polyhedron*., 2011, **30**, 123 – 131; (g) S. Anbu, M. Kandaswamy, M. Selvaraj, Polyhedron, 2012, **33**, 1-8; (h) S. Anbu, M. Kandaswamy, *Inorg.Chim.Acta*., 2012, **385**, 45– 52; (i) S. Anbu, M. Kandaswamy, S. Kamalraj, J. Muthumarry, B.Varghese, *Dalton Trans*., 2011, **40**, 7310 – 7318; (j) S. Anbu, S. Kamalraj, B.Varghese, J. Muthumary, M. Kandaswamy, *Inorg.Chem*., 2012, **51**, 5580– 5592.

15. (a) Y. C. Liu, Z. F. Chen, L. M. Liu, Y. Peng, X. Hong, B. Yang, H. G. Liu, H. Liang, C. Orvig, *Dalton Trans*., 2009, 10813-10823; (b) Z. F. Chen, Y. C. Liu, Y. Peng, X. Hong, H. H. Wang, M. M. Zhang, H. Liang, *J. Biol. Inorg. Chem*., 2012, **17**, 247-258.

16. D. D. Li, J. L. Tian, W. Gu, X. Liu, H. H. Zeng, S. P. Yan, *J. Inorg. Biochem*., 2011, **105**, 894-901.

17. P. R. Murray, E. J. Baron, M. A. Pfaller, F. C Tenover, R. H..Yolke, 1995. "*Manual of*

Clinical Microbiology", 6th ed. Mosby Year Book, London.

18. M. L. Gresa, R. Ortiz, L. Perello, J. Latorre, M. L. Gonzalez, S. G. Granda, M. P. Priede, E. Canton, *Journal of Inorganic Biochemistry.*, 2002, **92**, 65-74.
19. J. Manonmani, R. Thirumurugan, M. Kandaswamy, M. Kuppayee, S. S. S. Raj, M. N. Ponnuswamy, G. Shanmugam, H. K. Fun, *Polyhedron*., 2000, **19**, 2011-2018.
20. (a) P. Zanello, S. Tamburini, P. A. Vigato, G. A. Mazzocchin, *Coord. Chem. Rev.*, 1987, **77**, 165-273; (b) F. Azevedo, C. T. Carrondo, B. Caseto, M. Convery, D. Domingues, C. Freire, T. Durate, K. Neilson, C. Santos, *Inorg. Chim. Acta.*, 1994, **219**, 43-54; (c) A. Benzekeri, P. Dubourdeax, J. M. Latour, P. Rey, J. Laugier, *J. Chem. Soc, Dalton Trans.*, 1991, 3359-3365.
21. (a) J. M. Latour, D. Lamonsin, S. S. Tandon, *Inorg. Chim. Acta*, 1985, **107**, L1-L2; (b) G. C. Patterson, R. Holm, *Bioinorg. Chem.*, 1975, **4**, 257-275; (c) D. E. Fenton, R. L. Lintvedt, *J. Am. Chem. Soc.*, 1978, **100**, 6367-6375; (d) Y. Nishida, S. Kida, *J. Chem. Soc. Dalton Trans.,* 1986, 2633-2640; (e) E. L. Lintvedt, F. L. S. Kramer, *Inorg. Chem.*, 1983, **22**, 796-802.
22. (a) A. Wolfe, G. H. Shimmer, T. Meehan, *Biochemistry.*, 1987, **26**, 6392–6396.
23. (a) S. A. Tysoe, R. J. Morgan, A. D. Baker, T. C. Strekas, *J. Phys. Chem.*, 1993, **97**, 1707-1711; (b) J. M. Kelly, A. B. Tossi, D. J. McConnell, C. OhUigin, *Nucleic Acids Res.*, 1985, **13** 6017-6034; (c) I. S. Haworth, A. H. Elcock, J. Freemann, A. Rodger, W. G. J. Richards, *J. Biomol. Struct. Dyn.*, 1991, **9**, 23-44. (d) S.S. Mandal, U. Varshney, S. Bhattacharya, Bioconjugate Chem, 1997, 8, 798-812
24. A. Wolfe, G. H. Shimer, T. Mechan, *Biochemistry*., 1987, **26**, 6392-6396.
25. (a) A. M. Pyle, J. P. Rehmann, R. Meshoyrer, C. V. Kumar, N. J. Turro, J. K. Barton, *J. Am. Chem. Soc.*, 1989, **111**, 3051-3058; (b) L. Chen, J. Liu, J. Chen, C. Tan, *J. Inorg. Biochem.*,

2008, **102**, 330-341

26. (a) J. B. Lepecq, C. Paoletti, *J. Mol. Biol*. 1967, **27**, 87-106; (b) U. McDonnell, M. R. Hicks, M. J. Hannon, A. Rodger, *J. Inorg. Biochem*., 2008, **102**, 2052-2059.
27. S. S. Bhat, A. A. Kumbhar, H. Heptullah, A. A. Khan, V. V. Gobre, S. P. Gejji, V. G. Puranik, *Inorg. Chem*., 2011, **50**, 545–558.
28. M. Lee, A. L. Rhodes, M. D. Wyatt, S. Forrow, J. A. Hartley, *Biochemistry*., 1993, **32**, 4237–4245.
29. (a) W. Qian, F. Gu, L. Gao, S. Feng, D. Yan, D. Liao, P. Cheng, *Dalton Trans.*, 2007, 1060-1066; (b) Y. Zhao, J. Zhu, W. He, Z. Yang, Y. Zhu, Y. Li, J. Zhang, Z. Guo, *Chem. J. Eur.*, 2006, **12**, 6621-6629.
30. (a) K. Sato, M. Chikira, Y. Fujiib, A. Komatsu., *J. Chem. Soc., Chem. Commun*., 1994, 625-626; (b) M. Lee, A. L. Rhodes, M. D. Wyatt, S. Forrow, J. A. Hartley, *Biochemistry*., 1993, **32**, 4237–4245; (c) S. Ramakrishnan, D. Shakthipriya, M. A. Akbarsha, E. Suresh, V. S. Periasamy, M. Palaniandavar, *Inorg. Chem.,* 2011, **50**, 6458–6471.
31. D. G. Dalgleish, M. C. Feil, A. R. Peacocke, *Biopolymers*., 1972, **11**, 2415-2422.
32. F. Xue, C. Z. Xie, Y. W. Zhang, Z. Qiao, X. Qiao, J. Y. Xu, S. P. Yan., *J. Inorg. Biochem*., 2012, **115**, 78–86.
33. (a) W. Qian, F. Gu, L. Gao, S. Feng, D. Yan, D. Liao, P. Cheng, *Dalton Trans*., 2007, 1060–1066; (b) S. Anbu, M. Kandaswamy, P. Suthakaran, V. Murugan, B. Varghese, *J. Inorg. Biochem.,* 2009, **103**, 401–410.
34. Y. Hu, Y. Yang, C. Dai, Y. Liu, X. Xiao, *Biomacromolecules*, 2010, **11**, 106-112
35. (a) D. S. Raja, G. Paramaguru, N. S. P. Bhuvanesh, J. H. Reibenspies, R. Renganathan, K. Natarajan, *Dalton Trans.*, 2011, **40**, 4548-4559; (b) D. S. Raja, N. S. P. Bhuvanesh, K.

Natarajan, *Eur. J. Med. Chem.*, 2011, **46**, 4584-4594.

36. (a) A. Kathiravan, M. Chandramohan, R. Renganathan, S. Sekar, *J. Mol. Struct.*, 2009, **919**, 210-214; (b) J. R. Lakowicz, *Fluorescence quenching: Theory and Applications: Principles of Fluorescence Spectroscopy*, Kluwer Academic/Plenum Publishers, New York, 1999, 53–127.
37. T. Mosmann, *J. Immunology methods*., 1983, **65**, 55-63.
38. H. Arslan, N. Duran, G. Borekci, C. K. Ozer, C. Akbay, *Molecules.,* 2009, **14***,* 519-527.
39. M. Eweis, S. S. Elkholy, M. Z. Elsabee, *Int. J. Biol. Macromol.,* 2006, **38**, 1-8.
40. W. W, Navarre, O. Schneewind, *Microbiol. Mol. Biol. Rev.,* 1999, **63**, 174–229.